Mössbauer spectroscopy, magnetization, magnetic susceptibility, and low temperature heat capacity of α-Na_2NpO_4

Smith, Anna L.; Hen, Amir; Magnani, Nicola; Sanchez, Jean Pierre; Colineau, Eric; Griveau, Jean Christophe; Raison, Philippe E.; Caciuffo, Roberto; Konings, Rudy J M; Cheetham, Anthony K.

DOI
10.1088/0953-8984/28/8/086002

Publication date
2016

Document Version
Final published version

Published in
Journal of Physics: Condensed Matter

Mössbauer spectroscopy, magnetization, magnetic susceptibility, and low temperature heat capacity of α-Na_2NpO_4

OPEN ACCESS
IOP Publishing
Journal of Physics: Condensed Matter
J. Phys.: Condens. Matter **28** (2016) 086002 (11pp)
doi:10.1088/0953-8984/28/8/086002

Mössbauer spectroscopy, magnetization, magnetic susceptibility, and low temperature heat capacity of α-Na_2NpO_4

Anna L Smith,[1,2,5], Amir Hen[1], Nicola Magnani[1], Jean-Pierre Sanchez[3,4], Eric Colineau[1], Jean-Christophe Griveau[1], Philippe E Raison[1], Roberto Caciuffo[1], Rudy J M Konings[1] and Anthony K Cheetham[2]

[1] European Commission, Joint Research Centre (JRC), Institute for Transuranium Elements (ITU), PO Box 2340, D-76125 Karlsruhe, Germany
[2] Department of Materials Science and Metallurgy, University of Cambridge, 27 Charles Babbage Road, Cambridge CB3 0FS, UK
[3] CEA, INAC-SPSMS, FR-38000, Grenoble, France
[4] Université de Grenoble Alpes, INAC-SPSMS, FR-38000, Grenoble, France

E-mail: a.l.smith@tudelft.nl and eric.colineau@ec.europa.eu

Received 28 September 2015, revised 23 November 2015
Accepted for publication 7 December 2015
Published 29 January 2016

Abstract

The physical and chemical properties at low temperatures of hexavalent disodium neptunate α-Na_2NpO_4 are investigated for the first time in this work using Mössbauer spectroscopy, magnetization, magnetic susceptibility, and heat capacity measurements. The Np(VI) valence state is confirmed by the isomer shift value of the Mössbauer spectra, and the local structural environment around the neptunium cation is related to the fitted quadrupole coupling constant and asymmetry parameters. Moreover, magnetic hyperfine splitting is reported below 12.5 K, which could indicate magnetic ordering at this temperature. This interpretation is further substantiated by the existence of a λ-peak at 12.5 K in the heat capacity curve, which is shifted to lower temperatures with the application of a magnetic field, suggesting antiferromagnetic ordering. However, the absence of any anomaly in the magnetization and magnetic susceptibility data shows that the observed transition is more intricate. In addition, the heat capacity measurements suggest the existence of a Schottky-type anomaly above 15 K associated with a low-lying electronic doublet found about 60 cm^{-1} above the ground state doublet. The possibility of a quadrupolar transition associated with a ground state pseudoquartet is thereafter discussed. The present results finally bring new insights into the complex magnetic and electronic peculiarities of α-Na_2NpO_4.

Keywords: sodium neptunate, Mössbauer spectroscopy, magnetic susceptibility, magnetization, heat capacity

(Some figures may appear in colour only in the online journal)

[5] Current address: Delft University of Technology, Radiation Science & Technology Department, Nuclear Energy and Radiation Applications (NERA), Mekelweg 15, 2629 JB Delft, The Netherlands

1. Introduction

The ternary oxides of uranium, neptunium, and plutonium formed with sodium metal have been studied extensively since the 1960s because of their technological relevance for Sodium-cooled Fast Reactors (SFRs). In case of a clad breach of the stainless steel cladding, although extremely rare during normal operation, the sodium metallic coolant can come into contact with the (U,Np,Pu)O_2 fast reactor fuel, leading to the formation of sodium actinide oxide phases at the fuel-cladding interface [1, 2]. The latter phases show a lower density and lower thermal conductivity than the fuel [3–5], and therefore can induce local swelling and temperature increase in the fuel pin. The potential products of interaction are numerous, i.e. Na_2AnO_3, $NaAnO_3$, Na_3AnO_4, Na_2AnO_4, Na_4AnO_5, $Na_2An_2O_7$, Na_5AnO_6 (An = U,Np,Pu) [6–10], and the safety assessment of the fuel-sodium interaction therefore requires a comprehensive knowledge of their structural, thermomechanical, and thermodynamic properties.

In addition, the alkali metal and alkaline earth ternary actinide oxides have attracted in general a considerable interest as these 5*f* systems have shown exciting electronic and magnetic properties [11]. The 5*f* electrons of the actinides have a large spatial extension, by contrast with the 4*f* electrons of the lanthanides which are more core-like. The 5*f* valence shells are very close in energy to the 6*d*'s, and are therefore more prone to participate in chemical bonding. This specific feature allows on the one hand a wide range of oxidation states, between +3 and +7, and on the other hand the occurrence of various magnetic behaviours in these compounds. The theoretical description of these systems appears extremely challenging, however, as the crystal-field interaction is usually of the same order of magnitude as the spin–orbit coupling interaction, and electronic repulsion [12]. But in the case of the $[Rn]5f^1$ electronic configuration, corresponding to pentavalent uranium, hexavalent neptunium, or heptavalent plutonium, the contribution from electronic repulsion is removed, which simplifies greatly the interpretation.

One particularly interesting and intriguing phase is the hexavalent disodium neptunate, α-Na_2NpO_4, which was investigated in the present work using Mössbauer spectroscopy, magnetization, magnetic susceptibility, and heat capacity measurements at low temperatures. α-Na_2NpO_4, isostructural with α-Na_2UO_4 [13], has orthorhombic symmetry, in the space group *Pbam*, with lattice parameters $a = 9.715(3)$ Å, $b = 5.732(3)$ Å, $c = 3.459(3)$ Å according to powder x-ray diffraction studies [6]. Kanellakopulos and co-workers performed magnetic susceptibility measurements on this compound in 1980, which suggested an anomalous behaviour below 120 K, the magnetic interactions being likely antiferromagnetic [14]. The reported data showed an unexpected shape, however, which stimulated us to investigate more thoroughly the crystal chemistry and physical properties of α-Na_2NpO_4 at low temperatures.

The crystal structure was refined already by the Rietveld method [6], but the Np(VI) valence state in this phase, and therefore $[Rn]5f^1$ electronic configuration, was never confirmed. ^{237}Np Mössbauer spectroscopy is a very powerful technique for this purpose, which was used herein to verify the charge state. Mössbauer spectroscopy gives a direct insight into the electronic and local structural environment around the investigated nucleus, as well as the magnetic field acting on it [15]. The local structural properties around the neptunium cation as inferred from the x-ray diffraction refinement were hence related to the fitted Mössbauer parameters, i.e. quadrupole coupling constant and asymmetry parameters. In addition, magnetic hyperfine splitting was observed below 12.5 K, which could indicate magnetic ordering at this temperature. The magnetization and magnetic susceptibility results obtained herein show the interpretation is intricate, however. Finally, the heat capacity measurements revealed a λ-peak at 12.5 K and the occurrence of a Schottky-type anomaly above 15 K. The associated electronic entropy contributions were derived, and explanations for those features suggested.

2. Experimental methods

2.1. Sample preparation and powder x-ray diffraction

α-Na_2NpO_4 was prepared as described in [16] by solid state reaction between neptunium dioxide ($^{237}NpO_2$, ORNL, Oak Ridge) and sodium oxide (Na_2O 80% + Na_2O_2 20%, Alfa Aesar) mixed in stoichiometric amounts. The sample purity was checked using x-ray diffraction and ICP-MS analysis. The x-ray diffraction measurements were performed using a Bruker D8 x-ray diffractometer mounted in the Bragg-Brentano configuration, with a curved Ge monochromator (1 1 1), a copper tube (40 kV, 40 mA), and equipped with a LinxEye position sensitive detector. The data were collected by step scanning in the angle range $10° \leqslant 2\theta \leqslant 120°$, with an integration time of about 8 h, a count step of 0.02° (2θ), and a dwell of 5 s/step. Structural analysis was performed by the Rietveld method with the Fullprof2k suite [17]. No secondary phases were detected with this technique. The ICP-MS analysis moreover yielded a sodium to neptunium ratio of (2.01 ± 0.04)[6], indicating a mass fraction purity >0.99.

2.2. Mössbauer spectroscopy

The ^{237}Np Mössbauer spectroscopy measurements were carried out in transmission using an ^{241}Am metal source (∼108 mCi) with a sinusoidal driving mode. The effect was measured with a photon energy of 59.54 keV. The powder sample, encapsulated in three concentric aluminium containers, was measured in the temperature range 4.2–50 K, while the source was kept at a constant temperature of 4.2 K inside an independent chamber in the stainless steel cryostat. The velocity scale was calibrated with respect to $NpAl_2$.

[6] The uncertainty is an expanded uncertainty $U = k.u_c$ where u_c is the combined standard uncertainty estimated following the ISO/BIPM Guide to the Expression of Uncertainty in Measurement. The coverage factor is $k = 2$.

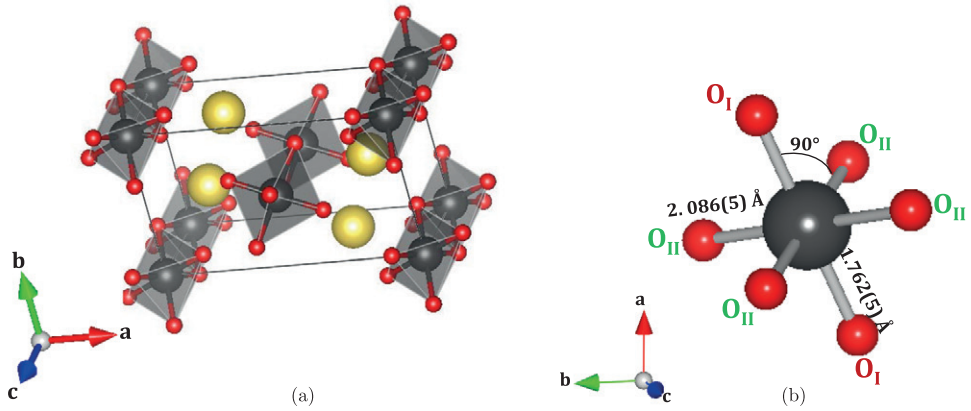

Figure 1. (a) Crystal structure of α-Na_2NpO_4 (Na atoms in yellow, O atoms in red, NpO_6 octahedra in gray) showing the edge-sharing of the NpO_6 octahedra along the c-axis. (b) NpO_6 octahedron in α-Na_2NpO_4 with the neptunyl type of coordination.

2.3. Magnetization and magnetic susceptibility measurements

Magnetization and magnetic susceptibility measurements were performed using a SQUID magnetometer (Quantum Design MPMS-7), at $\mu_0 H = 0$ to 6 tesla for $T = 3.5$, 4.2, 5, 10, 19.3, 50, and 100 K, as well as from 3.5 to 301 K, in a field of $\mu_0 H = 0.1$, 1, and 5 tesla, respectively. The magnetic susceptibility data were corrected for diamagnetism of the constituents (by subtracting $(-M_{Na2NpO4}/2 \cdot 10^{-6}$ emu·mol^{-1} from the collected data, $M_{Na2NpO4}$ being the molar mass of the material).

The magnetic susceptibility curve $\chi_M(T)$ was fitted with a modified Curie–Weiss law (equation (1)):

$$\chi_M(T) = \chi_0^* + \frac{C^*}{T - \theta_P} \quad (1)$$

where χ_M is the molar magnetic susceptibility (in emu·mol^{-1}), χ_0^* a temperature independent contribution to the magnetic susceptibility, C^* the Curie constant of the material, and θ_P the Weiss constant.

The experimental parameters χ_0^* and C^* were renormalized according to Amoretti and Fournier [18]. The effective moment was derived from the relation $\mu_{eff}(\mu_B) = 2.828(C)^{1/2}$, where the renormalized Curie constant C and temperature independent contribution χ_0 equal:

$$C = \frac{(C^* - \theta_P \chi_0^*)^2}{C^*} \quad (2)$$

$$\chi_0 = \frac{\chi_0^*(C^* - \theta_P \chi_0^*)}{C^*}. \quad (3)$$

2.4. Low temperature heat capacity

Low temperature heat capacity data were collected with a PPMS (physical property measurement system, quantum design) instrument, in the temperature range 2.1–301 K in the absence of a magnetic field, and in the temperature range 7–30 K with a 7 and 14 tesla magnetic field. This technique is based on a relaxation method, which was critically assessed by Lashley *et al* [19]. The measurements were carried out on 17.83(5) mg of α-Na_2NpO_4 material encapsulated in Stycast 2850 FT, and the heat capacity contribution of the Stycast subtracted from the recorded data. A more detailed description of the experimental procedure, which is particularly well adapted to the study of radioactive materials, was given in [20]. The contribution of the sample platform, wires, and grease was also deduced by a separate measurement of an addenda curve. Based on the experience acquired on this instrument with standard materials and other compounds [19, 20], the uncertainty was estimated at about 1% in the middle range of acquisition (10–100 K), and reaching about 3% at the lowest temperatures and near room temperature.

3. Results and discussion

3.1. Mössbauer spectroscopy

The crystal structure of α-Na_2NpO_4 is made of infinite chains along the c-axis of edge-sharing NpO_6 octahedra (figure 1(a)). The sodium atoms are located in between the chains and bind them together. Moreover, the NpO_6 octahedra show a neptunyl type of coordination, with two short Np-O_I bonds at 1.762(5) Å in the axial direction, and four long Np-O_{II} bonds at 2.086(5) Å in the equatorial plane [6] (figure 1(b)). The intrachain and interchain Np-Np distances are 3.459(5) Å and 5.640(5) Å, respectively. The neptunyl type of configuration is also found in β-Na_2NpO_4 (orthorhombic symmetry, in space group *Pbca*), but in no other composition among the series of sodium neptunate phases [6]. However, it is quite common among hexavalent alkali metal actinide oxide phases [21]. It is found in K_2UO_4 [22] and K_2NpO_4 [23] (tetragonal symmetry, in space group *I*4/*mmm*), in $BaUO_4$ [22] and $BaNpO_4$ [24] (orthorhombic symmetry, in space group *Pbcm*).

Mössbauer spectra of α-Na_2NpO_4 were collected at several temperatures between 4.2 and 50 K. Figure 2 shows selected Mössbauer spectra. The spectrum at 20 K consists of a single quadrupolar split pattern centered at -37.3 mm·s^{-1}, which corresponds to an isomer shift value as $\delta_{IS} = -50.9(3)$ mm·s^{-1} relative to the standard $NpAl_2$ absorber. The latter lies in the range $-32 < \delta_{IS} < -62$ mm·s^{-1}, which confirms the Np(VI)

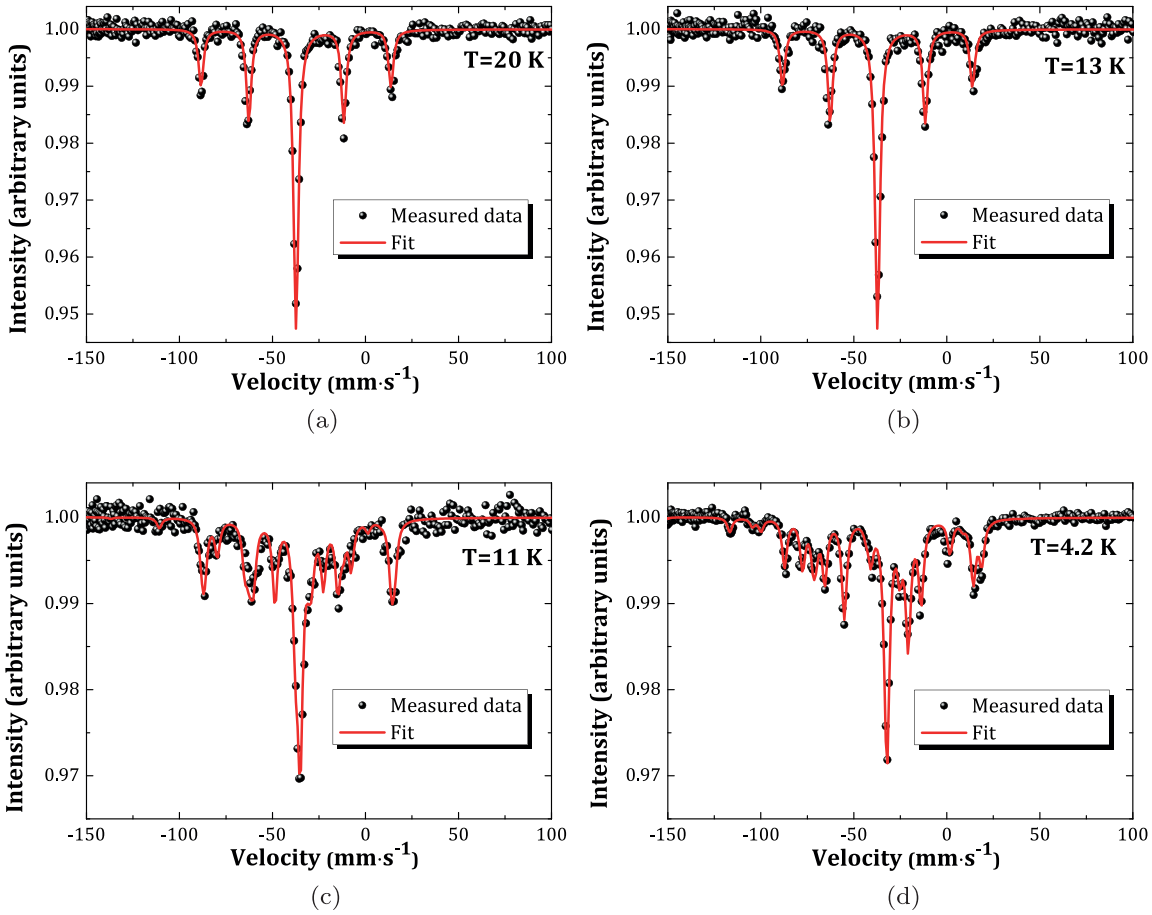

Figure 2. Mössbauer spectra of α-Na_2NpO_4 collected at selected temperatures and fit to the data.

charge state, corresponding to a $[Rn]5f^1$ electronic configuration, as displayed in the correlation diagram in figure 3. The Np ion in this structure is therefore a Kramers ion with a $^2F_{5/2}$ ground state manifold, and $^2F_{7/2}$ first excited state arising from spin–orbit coupling.

Fitted Mössbauer parameters are valuable information that can be related to the local structural environment around the neptunium cation. In particular, the absence of an asymmetry parameter for this structure, i.e. $\eta = 0$, is directly related to the axial symmetry of the NpO_6 octahedra. Moreover, the large value of the quadrupole coupling constant, i.e. $|e^2qQ| = 170.6(3)$ mm·s^{-1}, comes from the $(NpO_2)^{2+}$ neptunyl type of ions, and is attributed essentially to the contribution of the bonding electrons to the electric field gradient [26]. Quadrupole coupling constant values around 100 mm·s^{-1} were also reported for K_2NpO_4 [23], and β-Na_2NpO_4 [21]. By contrast, Na_4NpO_5 and Li_4NpO_5, which contain slightly elongated octahedra in a 'reverse' neptunyl type of configuration (with two long distances in the axial direction, and four short bonds in the equatorial plane), show much smaller values of the quadrupole coupling constant (around 15 mm·s^{-1}) [8, 21, 27].

Jové *et al* pointed out the existence of a linear relationship between the average neptunium-ligand distance and isomer shift for hexavalent neptunium compounds [21, 27]. The values reported herein for α-Na_2NpO_4 do not fit into this trend, however, as shown in figure 4. The mean Np-O distances for Li_4NpO_5 [30], K_2NpO_4 [31], β-Na_2NpO_4 [6, 13], and Ba_2CoNpO_6 [34, 35] have been updated in this figure compared to the figure of Jové *et al* [27]. In addition, the negative value of the quadrupole coupling constant e^2qQ (see table 1) is also very surprising, as hexavalent neptunium compounds usually show a positive value [21, 27]. α-Na_2NpO_4 presents a structural peculiarity, which is worth pointing out. Considering uranate phases with an uranyl ion, i.e. K_2UO_4 (U-2O_I = 1.913(6) and U-4O_{II} = 2.1661(1) Å [22]), β-Na_2UO_4 (U-2O_I = 1.913(2), U-2O_{II} = 2.178(3) Å, and U-2O_{II} = 2.180(3) Å [13]), α-Na_2UO_4 (U-2O_I = 1.903(2) and U-4O_{II} = 2.191(1) Å [13]), and $BaUO_4$ (U-2O_I = 1.872(12), U-2O_{II} = 2.196(6) Å, and U-2O_{II} = 2.223(6) Å [36]), it appears that a decrease of the axial U-O_I distance leads to an increase of the equatorial U-O_{II} distances. By contrast, in α-Na_2NpO_4, a decrease in the axial Np-O_I distance leads to a decrease of the equatorial Np-O_{II} bond length. The isomer shift value, which stands outside of the linear trend, and the negative value of the quadrupole coupling constant could be related to this particularity.

The Mössbauer spectrum recorded at 4.2 K is very different from those collected above 12.5 K. This can be accounted for by diagonalization of the full magnetic plus quadrupole Hamiltonian in the effective field approximation. The isomer

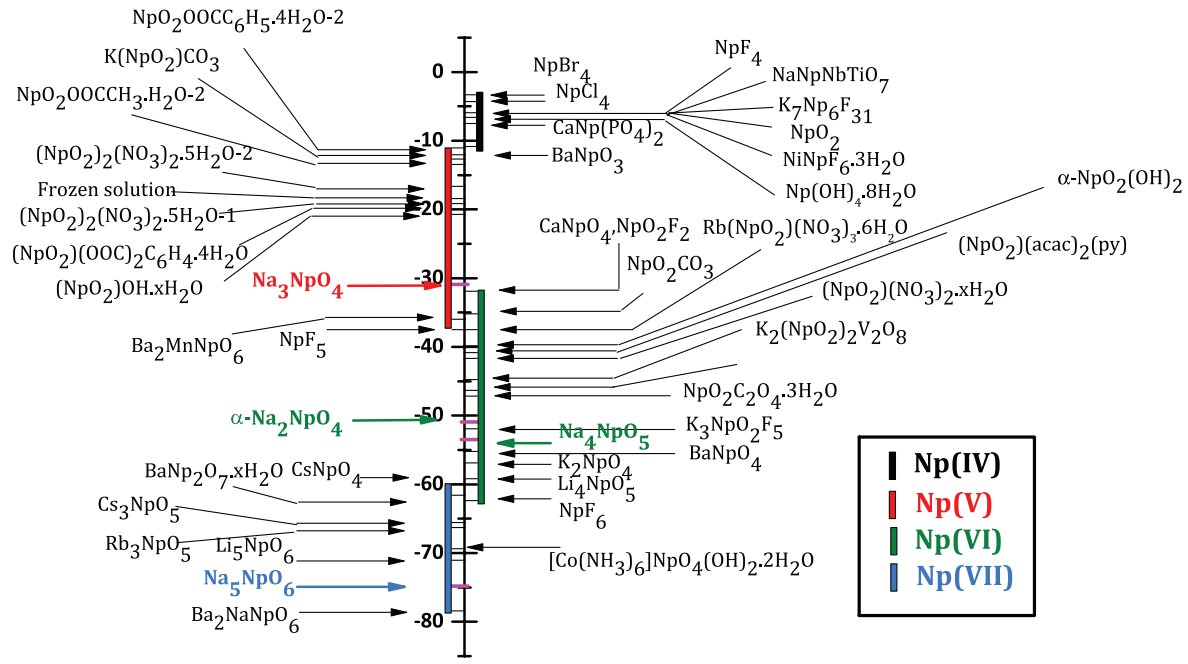

Figure 3. Isomer shifts versus $NpAl_2$ of Np(IV), Np(V), Np(VI), and Np(VII) compounds after [25]. The present result for α-Na_2NpO_4 is shown in green together with that for Na_3NpO_4 (red) [9], Na_4NpO_5 (green) [8] and Na_5NpO_6 (blue) [8].

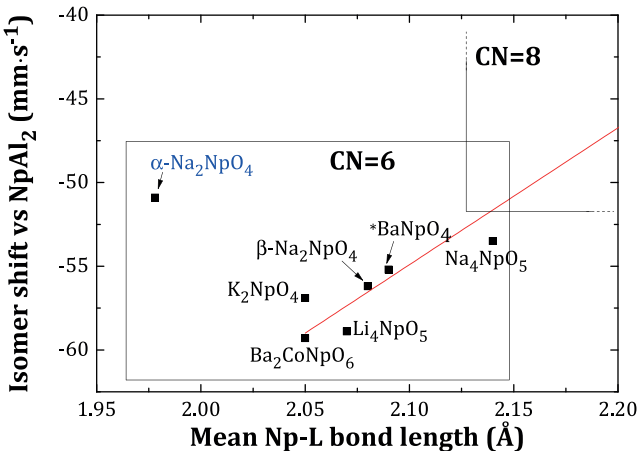

Figure 4. Isomer shift versus mean neptunium-ligand (Np-L) distance for selected hexavalent neptunium compounds in coordination (CN) 6. *When not available, the mean (Np-L) distance was approximated with the mean (U-L) distance reported by Jové *et al* [21] and was corrected for the difference in ionic radius between Np^{6+} and U^{6+} according to Shannon's tabulated data [37], i.e. 0.01 Å.

shift, quadrupole coupling constant, and asymmetry parameters are very close to the ones at 20 K. The magnetic field amounts to 105.3(3) T, a value in the same order of magnitude (~100 T) as reported for other 6-fold coordinated ternary oxides [21, 27]. The magnetic field is moreover found to be in the basal plane ($\theta = 90(2)°$), i.e. it makes an angle of 90° with respect to the principal axis of the electric field gradient which is along the axis of the $(NpO_2)^{2+}$ ion. This orientation is uncommon. Indeed, in Np(VI) neptunyl complexes, the field is usually found to be collinear with the neptunyl axis as the $(NpO_2)^{2+}$ ions are essentially isolated. The magnetic anisotropy is mainly determined by the second order B_2^0 crystal (ligand) field term which is negative, and the ground state is close to a pure $|\pm\frac{5}{2}>$ state [38]. Higher crystal field terms (i.e. B_4^0) come into interplay in the neptunates, however, and the magnetic anisotropy can be either along the neptunyl axis as in K_2NpO_4, or perpendicular to it as in the case of α-Na_2NpO_4. Here again, the peculiar bonding properties of the latter compound, as shown by the anomalous isomer shift and negative e^2qQ, seem to be responsible for the observed anisotropy.

Figure 5 shows the temperature dependence of the magnetic hyperfine field B_{hf} fitted with a Brillouin function ($J = 1/2$). These data show a critical temperature of 12.5 K, defining the limit between the temperature range where magnetic hyperfine splitting is observed (below 12.5 K), and the temperature range where only quadrupolar split spectra are observed (above 12.5 K). A priori, this particular feature can be explained in two ways: either the occurrence of a magnetic ordering transition at 12.5 K, or the indication of a slow electron spin relaxation phenomenon in a paramagnetic system [39]. However, the latter scenario can be ruled out as it implies an uncommon sudden collapse of the relaxation time at the critical temperature, i.e., a transition from a slow to a fast relaxation regime above 12.5 K. Moreover, the temperature dependence of B_{hf} is typical of those observed for an exchange split Kramers doublet. In addition, if the ground state doublet, as suggested below, is a $|\frac{5}{2}, \pm\frac{1}{2}>$ state, the relaxation is expected to be fast ($\Delta J_z = \pm 1$).

Finally, the fitted hyperfine field corresponds to an ordered moment (m) at 4.2 K of ~0.5 μ_B ($B_{hf}/m = (215T)\mu_B^{-1}$[7] [40]). The magnetic moments associated with a $|\frac{5}{2}, \pm\frac{5}{2}>$ and

[7] The original simple relation which holds between the hyperfine field (B_{hf}) and the ordered moment (m) determined by neutron diffraction was updated for the new value for the ground state nuclear moment $\mu_g = 2.5\mu_N$ [28, 29].

Table 1. Structural and Mössbauer parameters for some alkali hexavalent neptunates.

Phase	Bond lengths (Å)	Reference	δ_{IS}/$NpAl_2$ ($mm{\cdot}s^{-1}$)	e^2qQ ($mm{\cdot}s^{-1}$)	η	B_{hf}(T)	θ (°)	Reference
Na_4NpO_5	$Np\text{-}O_I = 2.06(\times 4)$ $Np\text{-}O_{II} = 2.31(\times 2)$	[8]	−53.5(3)[a]	10.5(3)[d]	0	—	—	[8]
Li_4NpO_5	$Np\text{-}O_I = 2.00(\times 4)$ $Np\text{-}O_{II} = 2.21(\times 2)$	[30]	−58.9(3)[b]	18[d]	0	—	—	[21, 27]
α-Na_2NpO_4	$Np\text{-}O_I = 1.762(\times 2)$ $Np\text{-}O_{II} = 2.086(\times 4)$	[21]	−51.0(3)[a]	−170.6(3)	0	105.3(3)	90(2)	This work
K_2NpO_4	$Np\text{-}O_I = 1.84(\times 2)$ $Np\text{-}O_{II} = 2.15(\times 4)$	[31]	−56.9(6)[a]	+88	0	122[c]	0	[21, 23]
$BaNpO_4$	$Np\text{-}O_I = 1.86(\times 2)$ $Np\text{-}O_{II} = 2.19(\times 2)$ $Np\text{-}O_{III} = 2.22(\times 2)$	[21, 27]	−54(2)[b]	+105.3(4)	0.37(3)	—	—	[32]
β-Na_2NpO_4	$Np\text{-}O_I = 1.90(\times 2)$ $Np\text{-}O_{II} = 2.16(\times 2)$ $Np\text{-}O_{III} = 2.17(\times 2)$	[6, 13]	−56.2(3)[b]	103.2(3)[d]	0	—	—	[33]

[a] IS value at 4.2 K.
[b] IS value at 77 K.
[c] Updated value for the ground state nuclear moment $\mu_g = 2.5\mu_N$ [28, 29].
[d] Sign unknown.

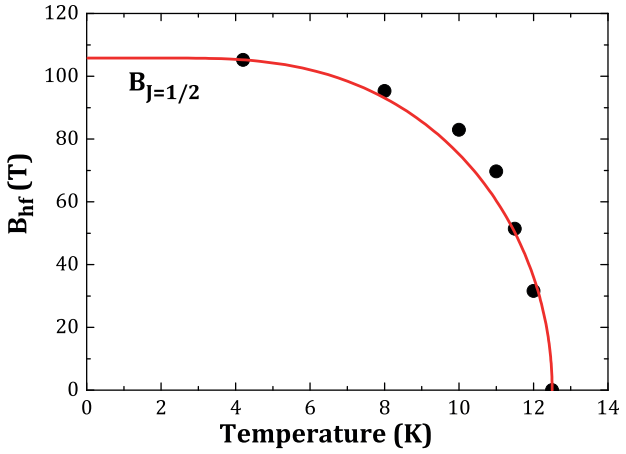

Figure 5. Variation of the magnetic hyperfine field B_{hf} (•) as a function of temperature. The red solid line is a fit of the data using a Brillouin function ($J = 1/2$).

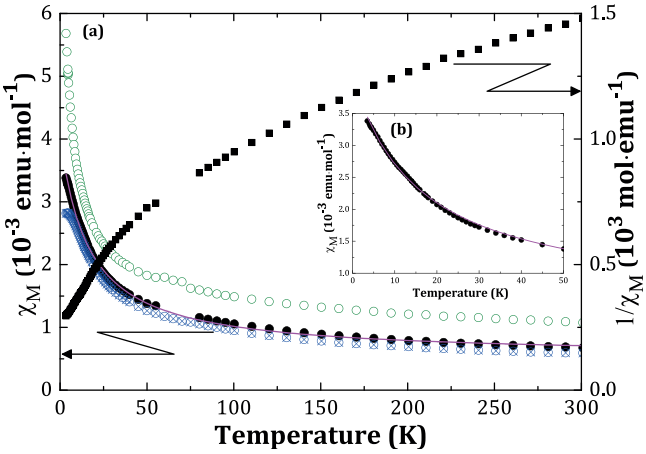

Figure 6. (a) Magnetic suceptibility of α-Na_2NpO_4 (•) and inverse susceptibility (■) as a function of temperature measured at $\mu_0 H = 5$ tesla. The pink line shows the modified Curie–Weiss fit on the present data. Magnetic susceptibility data collected at $\mu_0 H = 1$ tesla (○), and corrected for the ferromagnetic contribution (⊗).
(b) Magnetic susceptibility of α-Na_2NpO_4 collected below 50 K at $\mu_0 H = 5$ tesla and fit to the data using the modified Curie–Weiss law.

$|\frac{5}{2}, \pm\frac{1}{2}>$ ground states are 2.14 μ_B, and 0.57 μ_B, respectively. The low moment value in α-Na_2NpO_4 could therefore suggest a $|\frac{5}{2}, \pm\frac{1}{2}>$ ground state doublet. This is only a crude approximation, however, since the intermultiplet mixing as well as the covalency effects are not taken into account. The actual ground state could be more intricate. Magnetization and magnetic susceptibility measurements were carried out, as detailed in the next section, in an attempt to obtain a better insight into the origin of the anomaly observed at 12.5 K.

3.2. Magnetization and magnetic susceptibility

The magnetic susceptibility $\chi_M(T)$ of α-Na_2NpO_4 exhibits paramagnetic behaviour from room temperature down to 3.1 K (figure 6). Surprisingly, the collected data did not show any anomaly around 12.5 K, as could be expected from the Mössbauer results.

The compound's magnetic susceptibility was already measured in 1980 from 4.2 to 300 K by Kanellakopulos *et al* [14]. The reported data show a very large and flat maximum at about 50 K, a sharp minimum at 7 K, and an inflexion point at 12 K [11, 14, 41]. The authors interpreted this anomalous behaviour as a magnetic ordering transition, most probably of the antiferromagnetic type. But, the shape of their anomaly is

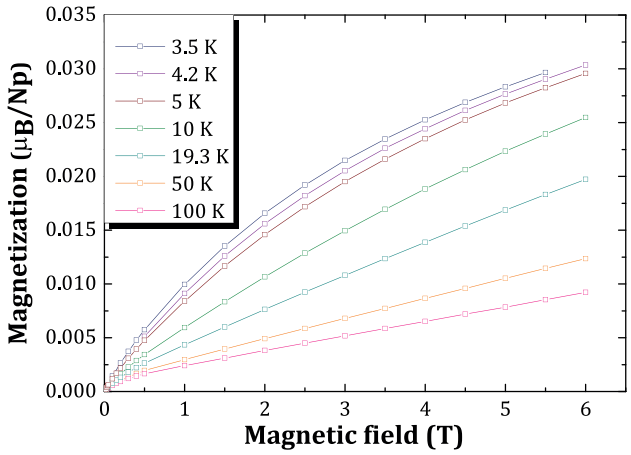

Figure 7. Magnetization curves recorded between 0 and 6 tesla for various temperatures.

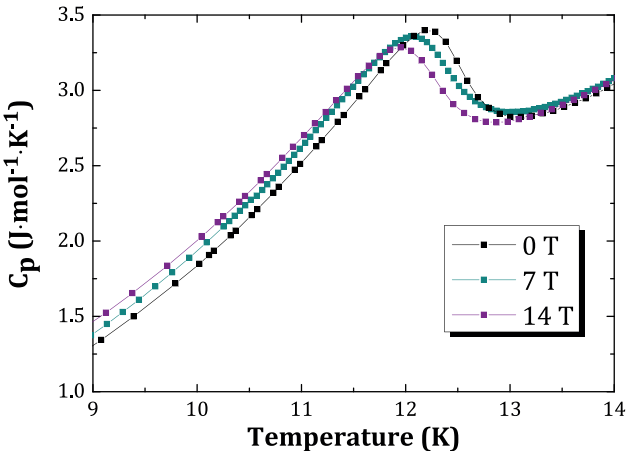

Figure 8. Heat capacity of α-Na_2NpO_4 in 0, 7, and 14 tesla magnetic field.

unusual, and could possibly come from reorientation of the sample in the Faraday balance.

The magnetization curves recorded in the present work for various temperatures as a function of the magnetic field did not show any anomaly at 12.5 K either (figure 7). However, a careful look at the data, especially those collected at 50 and 100 K, shows that the linear extrapolation of the corresponding curves does not go through zero at $\mu_0 H = 0$ T. This could indicate the presence of a small amount of ferromagnetic impurity. The associated magnetization is saturated at magnetic fields above about 0.5 T. The value of the magnetization ($\sim$0.03 μ_B) at 6 T and 3.5 K is much smaller than the ordered moment ($\sim$0.5 μ_B) deduced from the Mössbauer hyperfine field. This suggests that α-Na_2NpO_4, if ordered, would be an antiferromagnet. The curvature of the magnetization curves collected below 12.5 K could be due to a small canting of the antiferromagnetically coupled moments or alternatively to the presence of a small amount of paramagnetic moments (impurities or Np moments which avoid antiferromagnetic coupling). This latter possibility could explain why the intrinsic antiferromagnetic behaviour is masked.

The data $\chi_M(T)$ collected herein with an applied magnetic field of 5 tesla were fitted with a modified Curie–Weiss law (equation (1)) in the temperature range 3.5–301 K, yielding a temperature independent contribution to the magnetic susceptibility $\chi_0^* = 5.31(9) \cdot 10^{-4}$ emu·mol^{-1}, $C^* = 5.61(8) \cdot 10^{-2}$ emu·K·mol^{-1}, and $\theta_P = -15.8(3)$ K. Although no anomaly is observed in $\chi_M(T)$, the negative sign of the Weiss constant suggests the presence of antiferromagnetic interactions. The effective moment inferred from the data after renormalisation based on the method of Amoretti and Fournier [18], $\mu_{eff} = 0.77$ μ_B, is smaller than the value expected for the free Np^{6+} ion (2.54 μ_B in Russell-Saunders coupling using the free-ion J-value of the ground $^2F_{5/2}$ multiplet, $g_J = 6/7$). This is a general observation for alkali metal actinide ternary oxides with a $[Rn]5f^1$ central ion, where ligand fields effects are as important as spin–orbit effects. Repeating the magnetic susceptibility calculations of Kanellakopulos *et al* [14] (which reproduced very well their experimental results at high temperatures) using the same spin–orbit and crystal-field parameters, but without accounting for covalency (i.e. using $k = k' = 1$), yields for the ground state Γ_7 doublet an effective magnetic moment $\mu_{eff} = 0.81$ μ_B. The good agreement with our low temperature experimental data allows one to infer that the ligand-field potential is largely responsible for the effective moment reduction.

It is interesting to compare the present results with those obtained on K_2NpO_4 by Nectoux *et al* [23] and Jové *et al* [42], who performed Mössbauer spectroscopy and magnetic susceptibility measurements [23]. The K_2NpO_4 structure is made of a 2D network of infinite sheets with corner sharing NpO_6 octahedra [22]. The Mössbauer studies revealed magnetic hyperfine splitting at 19.5(5) K, with an associated hyperfine field of 122 tesla (table 1), corresponding to an ordered moment of about 0.6 μ_B, while the magnetic susceptibility curve did not show any anomaly in these ranges of temperature. Nectoux *et al* interpreted the Mössbauer results in terms of a first-order magnetic transition, probably associated with Jahn-Teller deformation. But the authors also pointed to the need for neutron diffraction data to confirm this hypothesis.

3.3. Heat capacity at low temperatures

The low temperature heat capacity data collected for α-Na_2NpO_4 show an anomaly at 12.5 K [43], which is shifted to slightly lower values when a magnetic field is applied as shown in figure 8. This critical temperature matches the one found by Mössbauer spectroscopy.

The excess electronic contribution to the heat capacity of α-Na_2NpO_4 was derived in this study in an attempt to obtain a better insight into the origin of the anomaly. The lattice heat capacity contribution was approximated with the one of α-Na_2UO_4 (which has electronic configuration $[Rn]5f^0$), as the two compounds are isostructural and have very similar atomic masses [44]. The difference between the two curves, shown in figure 9, corresponds to the electronic excess heat capacity.

This electronic contribution could correspond to an insulator-metal transition, a magnetic order-disorder transition, or a Schottky-type transition associated with low-lying electronic levels. An insulator-metal transition is ruled out in

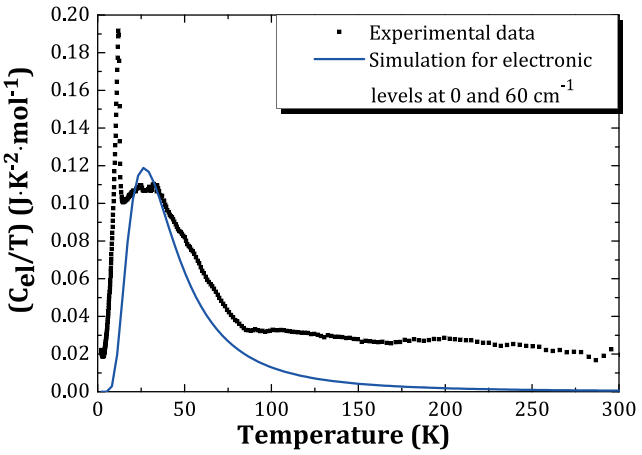

Figure 9. Electronic contribution to the heat capacity in α-Na_2NpO_4 obtained by subtracting the data reported for α-Na_2UO_4 [44] (■), and comparison with the simulation for energy levels at 0 and 60 cm^{-1} (blue line) using a Schottky function.

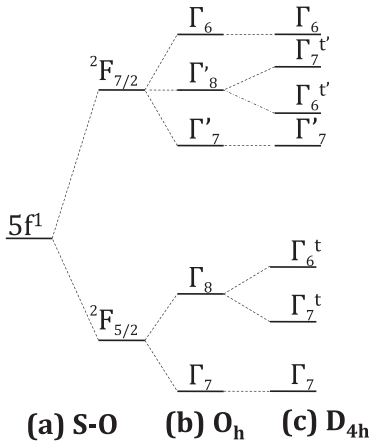

Figure 10. Splitting of the $5f^1$ electronic state by (a) spin–orbit coupling, (b) an O_h symmetry crystal field, and (c) a D_{4h} symmetry crystal field [52].

this case as α-Na_2NpO_4 is a forest green insulating material. For magnetic transitions, the electronic entropy, which is of a configurational nature, corresponds to the maximum disordering from an ordered magnetic structure, where all spins are oriented, to the disordered paramagnetic state, where all spins are degenerate [45]. The latter contribution is equal to $\Delta S_{magn} = R\ln(2S+1)$, where S is the total spin quantum number [45].

The curve obtained with this method shows a superposition of two different excess contributions. The first one at 12.5 K resembles a sharp λ peak associated with magnetic ordering, while the second one, with a very broad shape between 15 and 85 K, looks more like a Schottky-type anomaly. Above 100 K, the electronic heat capacity (C_{el}/T) reaches a constant value of about 0.025 $J{\cdot}K^{-2}{\cdot}mol^{-1}$, although it should reach zero (corresponding to the same lattice contribution at high temperatures for the uranium and neptunium compounds). But this discrepancy can be related on the one hand to the uncertainty on our experimental results which increases towards high temperatures using the PPMS technique, and on the other hand to the correction for the Stycast contribution.

The numerical integration of the $(C_{el}/T) = f(T)$ curve in the temperature range 2.1–15.3 K using the OriginPro software yielded $S_{\lambda peak} = 1.1\ J{\cdot}K^{-1}mol^{-1}$, i.e. about 19% of the expected order-disorder entropy for such a Kramers system ($S_{magn} = R\ln 2$), and $S_{Schottky} = 5.5\ J{\cdot}K^{-1}{\cdot}mol^{-1}$ for the Schottky-type anomaly integrated over the temperature range 15.3–88 K. The heat capacity data of α-Na_2NpO_4 and consequently the electronic heat capacity showed a slight re-increase below 3.7 K as visible in figure 11 and reported in [43]. Self-heating effects coming from the radioactive decay of ^{237}Np were considered, but appeared negligible [43]. The occurrence of a second transition below 2.1 K, possibly of magnetic nature, could be possible. Alternatively, this increase could arise from a nuclear Schottky effect due to the splitting of the $I = 5/2$ nuclear ground level of ^{237}Np nuclei by the hyperfine field and the quadrupolar interaction [43].

The entropy contribution of this slight raise is negligible and cannot explain the mismatch of $S_{\lambda peak}$ with the expected $R\ln 2$ value. The total excess entropy between 2.1 and 301 K was estimated as 12.2 $J{\cdot}K^{-1}{\cdot}mol^{-1}$, which is rather close to the entropy expected for the full Np $J = 5/2$ Hund's rule multiplet $R\ln 6$.

The λ-type feature at 12.5 K seems to be directly related to the magnetic hyperfine splitting observed at the same temperature by Mössbauer spectroscopy. Moreover, as the λ-peak is shifted to lower temperatures with the application of a magnetic field, one is tempted to interpret it as an antiferromagnetic ordering transition. The experimental magnetic entropy, i.e. 1.1 $J{\cdot}K^{-1}mol^{-1}$, is much lower than expected, but this is not uncommon for compounds where the 5*f* electrons participate to the chemical bonding [43] or are of itinerant character as in some intermetallic compounds [46]. The absence of any anomaly at 12.5 K in the magnetic susceptibility data is puzzling, however. Neutron diffraction measurements are required to confirm the existence of an antiferromagnetic state at low temperatures and to solve these apparently contradictory results.

As for the Schottky-type anomaly, this appears to be a rather recurrent feature among the family of sodium actinates with $[Rn]5f^1$ central ion. It was reported already for Na_4NpO_5 [8] and $NaUO_3$ [47]. Na_4NpO_5 adopts a paramagnetic behaviour over the whole temperature range according to Mössbauer spectroscopy and magnetic susceptibility data, and its low temperature heat capacity shows a broad Schottky-type anomaly between 3 and 15 K.

$NaUO_3$ was reported to be an antiferromagnet with a transition temperature at ~32 K as found in magnetic susceptibility, electron spin resonance, and neutron diffraction experiments [48–50]. Neutron diffraction measurements moreover indicated an orthorhombic magnetic cell, and a G-type antiferromagnetic ordering [50]. Interestingly, Lyon *et al*, who performed heat capacity measurements at low temperatures [47], found two types of excess electronic contributions as in the present case: a clear λ type anomaly associated with antiferromagnetic ordering, and Schottky-type feature above the lambda transition.

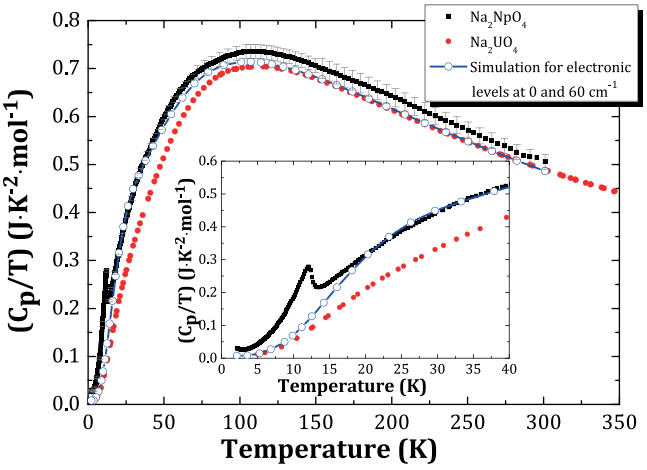

Figure 11. C_p/T against temperature for α-Na_2NpO_4 (present work) (■) and α-Na_2UO_4 reported by Osborne *et al*. [44] (•). Comparison with the sum of the lattice contribution of α-Na_2UO_4 and excess electronic entropy obtained by simulating energy levels at 0 and 60 cm^{-1} (○) using a Schottky function.

In the $[Rn]5f^1$ electronic configuration of α-Na_2NpO_4, the $^2F_{5/2}$ ground state has a degeneracy of $(2J+1)=6$, and is therefore split into three Kramers doublets (Γ_7 ground state, and Γ_7^t, Γ_6^t excited states) by the crystal field effect in the tetragonally distorted symmetry [11], as shown in the splitting scheme in figure 10. The $^2F_{7/2}$ level is split into four Kramers doublets. Volkovich *et al* assigned a D_{2h} crystal field symmetry to the isostructural α-Na_2UO_4 compound using Raman and infrared spectroscopy [51]. However, the optical spectroscopy measurements and electronic level calculations presented in the literature for α-Na_2NpO_4 are based on a D_{4h} approximation [11, 14]. The present results have also been interpreted considering a D_{4h} crystal field symmetry, which is justified in view of the neptunyl type of arrangement around the neptunium cation.

The entropy associated with the Schottky anomaly, obtained after subtraction of the lattice contribution of α-Na_2UO_4, was found very close to that of a two levels system, i.e. $S_{schottky} = R\ln\left(1+\frac{g_0}{g_1}\right) = R\ln 2$ [53]. The electronic levels associated with the $^2F_{5/2}$ ground state were subsequently simulated using a simple two levels Schottky function as written in equation (4) [53]:

$$C_{Schottky} = R\left(\frac{\theta_S}{T}\right)^2 \frac{g_0}{g_1} \frac{\exp\left(\frac{\theta_S}{T}\right)}{\left(1+\frac{g_0}{g_1}\exp\left(\frac{\theta_S}{T}\right)\right)^2} \qquad (4)$$

where θ_S is the spacing between the two low-lying electronic levels expressed in K, g_0 and g_1 their respective degeneracy ($g_0/g_1 = 1$ in this case). θ_S is related to the energy separation ε_1 between the two levels via the formula $\theta_S = \varepsilon_1/k_B$, where k_B is Boltzmann constant equal to 1.380 6488·10^{-23} J·K^{-1}.

Figure 9 compares the experimental electronic heat capacity with the one calculated for two low-lying Kramers doublets with the same degeneracy at 0 and 60 cm^{-1} (i.e. 7.44 meV or 86.3 K). In figure 11, the heat capacity of α-Na_2NpO_4 is moreover compared with the sum of the lattice contribution of α-Na_2UO_4 and excess electronic entropy calculated with the Schottky function. The agreement is remarkably good above the λ transition. Our simulation therefore makes quite a strong case for the existence of a Schottky-type anomaly in the heat capacity.

Optical spectroscopy measurements on α-Na_2NpO_4 were performed by Kanellakopulos and co-workers in 1980, which revealed transitions at 8130, 9 615, 10 310, 12 500, and 15 150 cm^{-1} [14]. The authors assigned them to the Γ_6^t and Γ_7^t levels, and three nearest doublets of the $^2F_{7/2}$ levels, respectively. The hypothesis of a Γ_7^t doublet lying 60 cm^{-1} above the Γ_7 ground state doublet would therefore require a complete reevaluation of the spectroscopic data and calculations of Kanellakopulos *et al* [54], according to which the Γ_7 ground state is well isolated.

Supposing that the first excited doublet is much closer in energy to the Γ_7 ground state than calculated by Kanellakopulos *et al* [54] (an assumption which would naturally explain the Schottky-type anomaly), we can suggest yet an alternative explanation to the heat capacity and magnetic susceptibility results obtained herein. In such a scenario, the transition at 12.5 K could be related to the ordering of electric quadrupoles rather than magnetic dipoles. Several examples of quadrupolar transitions in lanthanide-based tetragonal systems showing two low-lying Kramers doublets forming a quasi-quartet have been reported in the literature [55, 56]. In the case of α-Na_2NpO_4, the O_{xz} and the O_{yz} quadrupoles are active when the two lowest Γ_7 and Γ_7^t doublets are populated. The latter two Kramers doublets which compose a ground pseudo-quartet cannot be split into singlets (as opposed to magnetic order, which would break time reversal symmetry). This has two consequences: firstly, the latter quadrupoles could drive the phase transition without triggering magnetic dipoles as a secondary order parameter, which would explain why no sign of the phase transition is visible in the magnetic susceptibility data; secondly, the entropy change associated with the transition should be much smaller than $R\ln 2$, which fits well with our experimental results. However, it is difficult to explain why no trace of the presence of a second, low-lying Kramers doublet just above the ground state is visible in our Mössbauer spectra above 12.5 K. It is also not clear how the quadrupoles would affect the slow relaxation below the ordering temperature. Complementary experimental investigations at low energy and theoretical calculations are therefore needed to elaborate on our results and to fully understand the nature of this transition.

4. Conclusions

The present work has revealed very complex properties for α-Na_2NpO_4 at low temperatures. Mössbauer spectroscopy measurements have firstly confirmed the Np(VI) charge state and $[Rn]5f^1$ electronic configuration from the isomer shift value $\delta_{IS} = -50.9(3)$ mm·s^{-1}/$NpAl_2$. The local structural environment around the Np cation has moreover been related to the fitted Mössbauer parameters: $\eta = 0$ due to the axial

symmetry in the NpO_6 octahedra, while the large value of the quadrupole coupling constant, $e^2qQ = -170.6(3)$ mm·s^{-1}, is related to the $(NpO_2)^{2+}$ neptunyl type of ion. The Mössbauer spectra collected below 12.5 K have shown magnetic hyperfine splitting, which could be related to a magnetic ordering transition at this temperature. This hypothesis is substantiated by the occurrence of a λ-peak at 12.5 K in the low temperature heat capacity data ($S_{magn} = 1.1$ J·K^{-1}mol^{-1}). But surprisingly, the magnetic susceptibility curve did not present any anomaly at 12.5 K, while the low temperature magnetization data could suggest the occurrence of an antiferromagnetic ordering. These results seem to indicate a rather exotic magnetic ordering behaviour, and it would be extremely interesting to collect neutron diffraction data to gain further insight into the origin of the transition. Finally, simulations have made quite a strong case for the existence of a Schottky-type anomaly in α-Na_2NpO_4, with a low-lying electronic doublet 60 cm^{-1} above the ground state doublet. Thereafter, the occurrence of a quadrupolar ordering transition associated with a ground state pseudoquartet has been postulated in this work to explain our experimental observations as an alternative to magnetic ordering. Such hypothesis would explain the small value of the entropy associated with the λ transition, the observation of a Schottky-type excess component, and the absence of any anomaly in the magnetic susceptibility data. However, more refined spectroscopic measurements at low energy are required to re-evaluate the Np(VI) crystal-field ground state and to conclude on the complex behaviour of α-Na_2NpO_4.

Acknowledgments

The authors would like to express their gratitude to D Bouëxière for the collection of room temperature x-ray data. They also thank the 7th Framework Program of the European Commission, and the Joint Advanced Severe Accidents Modelling and Integration for Na-cooled neutron reactors (JASMIN) programme (N°295803 in FP7). ALS acknowledges the European Commission and the Ras al Khaimah Centre for Advanced Materials for funding her PhD studentship.

References

[1] Keller C, Koch L and Walter K H 1965 *J. Inorg. Nucl. Chem.* **27** 1205–23
[2] Keller C, Koch L and Walter K H 1965 *J. Inorg. Nucl. Chem.* **27** 1225–32
[3] Blackburn P E and Hubbard W K 1972 *Proc. of Conf. on Fast Reactor Fuel Element Technology* ed R Farmakes (Hinsdale, IL: American Nuclear Society) p 479
[4] Housseau M, Dean G and Perret F 1974 *Behaviour and Chemical State of Irradiated Ceramic Fuels* (Panel Proc. Series) (Vienna: IAEA) p 349
[5] Housseau M, Dean G, Marcon J P and Marin J F 1973 *Report* CEA-N-1588 (Commissariat à l'énergie atomique et aux énergies alternatives)
[6] Smith A L, Raison P E and Konings R J M 2011 *J. Nucl. Mater.* **413** 114–21
[7] Smith A L *et al* 2015 *Inorg. Chem.* **54** 3552–61
[8] Smith A L, Hen A, Raison P E, Colineau E, Griveau J C, Magnani N, Sanchez J P, Konings R J M, Caciuffo R and Cheetham A K 2015 *Inorg. Chem.* **54** 4556–64
[9] Smith A L, Raison P E, Hen A, Bykov D, Colineau E, Sanchez J P, Konings R J M and Cheetham A K 2015 *Dalton Trans.* **44** 18370–7
[10] Bykov D, Raison P, Konings R J M, Apostolidis C and Orlova M 2015 *J. Nucl. Mater.* **457** 54–62
[11] Bickel M and Kanellakopulos B 1993 *J. Solid State Chem.* **107** 273–84
[12] Santini P, Carretta S, Amoretti G, Caciuffo R, Magnani N and Lander G H 2009 *Rev. Mod. Phys.* **81** 807–64
[13] Cordfunke E H P and IJdo D J W 1995 *J. Solid State Chem.* **115** 299–304
[14] Kanellakopulos B, Henrich E, Keller C, Baumgärtner F, König E and Desai V P 1980 *Chem. Phys.* **53** 197–213
[15] Kalvius G M, Dunlap B D, Asch L and Weigel F 2005 *J. Solid State Chem.* **178** 545–53
[16] Smith A L, Colle J Y, Beneš O, Kovacs A, Raison P E and Konings R J M 2013 *J. Chem. Thermodyn.* **60** 132–69
[17] Rodriguez-Carvajal J 1993 *Physica* B **192** 55–69
[18] Amoretti G and Fournier J M 1984 *J. Magn. Magn. Mater.* **43** L217–20
[19] Lashley J C *et al* 2003 *Cryogenics* **43** 369–78
[20] Javorský P, Wastin F, Colineau E, Rebizant J, Boulet P and Stewart G 2005 *J. Nucl. Mater.* **344** 50–5
[21] Jové J, Cousson A, Abazli H, Tabuteau A, Thévenin T and Pagès M 1988 *Hyp. Int.* **39** 1–16
[22] Roof I P, Smith M D and Zur Loye H C 2010 *J. Cryst. Growth* **312** 1240–3
[23] Nectoux F, Jové J, Cousson A, Pagès M and Gal J 1981 *J. Magn. Magn. Mater.* **24** L113–6
[24] Appel H, Bickel M, Melchior S and Kanellakopulos B 1990 *J. Less-Common Met.* **162** 323–34
[25] Yoshida Z, Johnson S G, Kimura T and Krsul J R 2006 ch 6, Neptunium *The Chemistry of the Actinide and Transactinide Elements* ed L R Morss *et al* (Dordrecht: Springer) pp 699–812
[26] Dunlap B D, Kalvius G M and Shenoy G K 1971 *Phys. Rev. Lett.* **26** 1085–8
[27] Jové J, Proust J, Pagès M and Pyykkö P 1991 *J. Alloys Compd.* **177** 285–310
[28] Ellis Y A 1978 *Nucl. Data Sheets* **23** 71–121
[29] Fuller G H 1976 *J. Phys. Chem. Ref. Data* **5** 835
[30] Morss L, Appelman E, Gerz R and Martin-Rovet D 1994 *J. Alloys Compd.* **203** 289–95
[31] Smith A L 2015 (unpublished results)
[32] Bickel M, Kanellakopulos B, Appel H, Haffner H and Geggus S 1986 *J. Less-Common Met.* **121** 291–9
[33] Jové J, Cousson A and Gasperin M 1986 *Hyp. Int.* **28** 853–6
[34] Hinatsu Y and Doi Y 2006 *J. Solid State Chem.* **179** 2079–85
[35] Tabuteau A and Pagès M 1985 *Handoook on the Physics and Chemistry of the Actinides* vol 3 ed A J Freeman and G H Lander (Amsterdam: North Holland) chapter 4
[36] Reis J A H, Hoekstra H R, Gebert E and Peterson S W 1976 *J. Inorg. Nucl. Chem.* **38** 1481–5
[37] Shannon R D 1976 *Acta Cryst.* A **32** 751–67
[38] Dunlap B D and Kalvius G M 1979 *J. Phys. Colloq.* **70** 192–3
[39] Dickson D P E and Berry F J 2005 *Mössbauer Spectroscopy* (New York: Cambridge University Press)
[40] Dunlap B D and Lander G H 1974 *Phys. Rev. Lett.* **33** 1046–8
[41] Bickel M 1986 Zusammenhang zwischen strukturellen und magnetischen Eigenschaften am Beispiel von sauerstoffhaltigen Verbindungen der Actinide *PhD Thesis* Institut für Heisse Chemie, Kernforschungszentrum Karlsruhe
[42] Jové J, Nectoux F, Tabuteau A and Pagès M 1981 *Proc. Int. Conf. on the Applications of the Mössbauer effect, Proc. of the Indian National Science Academy (Jaipur, India)* pp 580–2

[43] Smith A L, Griveau J C, Colineau E, Raison P and Konings R J M 2015 *Thermochim. Acta* **617** 129–35
[44] Osborne D W, Flotow H E, Dallinger R P and Hoekstra H R 1974 *J. Chem. Thermodyn.* **6** 751–6
[45] Stolen S, Grande T and Allan N L 2004 *Chemical Thermodynamics of Materials* (New York: Wiley)
[46] Sechovsky V and Havela L 1988 *Ferromagnetic Materials* vol 4, Elsevier edn (Amsterdam: North Holland) p 309
[47] Lyon W G, Osborne D W, Flotow H E and Hoekstra H R 1977 *J. Chem. Thermodyn.* **9** 201–10
[48] Miyake C, Fuji K and Imoto S 1977 *Chem. Phys. Lett.* **46** 349–51
[49] Miyake C, Kanamaru M, Anada H and Imoto S 1985 *J. Nucl. Sci. Technol.* **22** 653–57
[50] Van den Berghe S, Leenaers A and Ritter C 2004 *J. Solid State Chem.* **177** 2231–6
[51] Volkovich V A, Griffiths T R, Fray D J and Fields M 1998 *Vib. Spectrosc.* **17** 83–91
[52] Bickel M, Kanellakopulos B and Powietzka B 1991 *J. Less-Common Met.* **170** 161–9
[53] Gopal E S 1966 *Specific Heats at Low Temperatures* (New York: Plenum Press)
[54] Kanellakopulos B, Keller C, Klenze R and Stollenwerk A H 1980 *Physica* B **102** 221–5
[55] Indoh K, Onodera H, Yamauchi H, Kobayashi H and Yamaguchi Y 2000 *J. Phys. Soc. Japan* **69** 1978–81
[56] Jeevan H S, Geibel C and Hossain Z 2006 *Phys. Rev.* B **73** 020407